The Glutamine Side Chain at Position 91 on the β5a−β5b Loop of Human Immunodeficiency Virus Type 1 Reverse Transcriptase Is Required for Stabilizing the dNTP Binding Pocket

ARTICLE *in* BIOCHEMISTRY · AUGUST 2011

Impact Factor: 3.02 · DOI: 10.1021/bi200815e · Source: PubMed

8 AUTHORS, INCLUDING:

Awadhesh Mishra
Sam Higginbottom Institute of Agriculture, T…
529 PUBLICATIONS **7,739** CITATIONS
SEE PROFILE

Alok K Upadhyay
Fox Chase Cancer Center
14 PUBLICATIONS **132** CITATIONS
SEE PROFILE

Thomas Comollo
Rutgers New Jersey Medical School
1 PUBLICATION **2** CITATIONS
SEE PROFILE

Neerja Kaushik-Basu
Rutgers New Jersey Medical School
41 PUBLICATIONS **658** CITATIONS
SEE PROFILE

Published in final edited form as:
Biochemistry. 2011 September 20; 50(37): 8067–8077. doi:10.1021/bi200815e.

Glutamine side chain at position 91 on the β5a-β5b loop of Human Immunodeficiency Virus Type 1 Reverse Transcriptase is required for stabilizing the dNTP binding pocket

Nootan Pandey[1,†], **Chaturbhuj A. Mishra**[1,†], **Dinesh Manvar**[1], **Alok K. Upadhyay**[1], **Tanaji T. Talele**[2], **Thomas W. Comollo**[1], **Neerja Kaushik-Basu**[1], and **Virendra N. Pandey**[1,*]

[1]Department of Biochemistry and Molecular Biology, UMD-New Jersey Medical School 185 South Orange Ave Newark, NJ 07103

[2]Department of Pharmaceutical Sciences, College of Pharmacy and Allied Health Professions, St. John's University, 8000 Utopia Parkway, Queens, NY 11439

Abstract

Earlier, we postulated that Gln91 of HIV-1 RT stabilizes the side chain of Tyr183 via hydrogen bonding interaction between O(H) of Tyr183 and CO of Q91 (Harris et al., BIOCHEMISTRY 37: 9630, 1998). To test this hypothesis, we generated mutant derivatives of Gln91 and analyzed their biochemical properties. The efficiency of reverse transcription was severely impaired by nonconservative substitution from Gln→Ala, while conservative substitution from Gln to Asn resulted in approximately 70% loss of activity, a value similar to that observed with Y183F mutation. The loss of polymerase activity of both Q91A and Q91N was significantly improved by Met to Val substitution at position 184. Curiously, the Q91N mutant exhibited stringency in discriminating between correct and incorrect nucleotides, suggesting its possible interaction with residues influencing the flexibility of the dNTP binding pocket. In contrast, both double mutants, Q91A/M184V and Q91N/M184V, are found to be as error prone as the wild-type enzyme. We propose a model that suggests that subtle structural changes in the region due to mutation at position 91 may influence the stability of the side chain of Tyr183 in the catalytic YMDD motif of the enzyme and thus altering the active site geometry that may interfere in the substrate recognition.

The rapid emergence of human immunodeficiency virus-1 (HIV-1) strains that are resistant to specific inhibitors has frustrated all efforts to control the spread of acquired immunodeficiency syndrome. The dynamics of HIV-1 replication *in vivo* have demonstrated that within 2–4 weeks after treatment with nucleoside analogs, the wild-type virus in plasma is completely replaced by drug-resistant mutants (1, 2). Virally encoded reverse transcriptase, which is essential for viral replication and establishing infection, efficiently converts the single-stranded HIV-1 viral RNA genome into the double-stranded proviral DNA. The functional form of mature HIV-1 RT contains two subunits, p66 and p51; the smaller subunit is derived from proteolytic cleavage of the larger subunit. Several high-resolution crystal structures of HIV-1 RT in apocrystal form, liganded with inhibitors and bound with DNA, as well as enzyme-DNA-dNTP ternary complex are now available (3–10). In the crystal structure, the polymerase domain of the larger subunit is folded into an open conformation containing the polymerase active site cleft, while the inert smaller subunit is closed and compact (8). The polymerase cleft resembles an open right hand that folds into

*Corresponding author: Virendra N Pandey, Ph.D. Tel.: 973-972-0660; FAX: 973-972-8657, pandey@umdnj.edu.
†Equal contribution

finger, palm, and thumb subdomains. Many amino acid residues in the polymerase domain of this enzyme have been subjected to extensive mutagenesis (11–17). A few of them have been subjected to in-depth biochemical characterization in order to define their functional roles in catalysis as well as in conferring drug resistant phenotypes (18–20). The mutant derivatives of amino acid residues at positions 65, 72, 89, 110, 115, 151, 160, 183, 184, 185, 186, 219, 249, 307, and 311, as well as most of the residues in Motif-E (residues 227–237) and the thumb subdomain (residues 253–271) have been extensively characterized and their functions in the context of three-dimensional (3-D) structure have been proposed (21–46).

We have extensively analyzed the mutant derivatives of catalytically important residues of the YMDD motif and proposed their functional role in the 3-D context (21, 26, 29, and 47). One residue in this motif that has been studied in detail is tyrosine, at position 183 (47). A conservative substitution of Tyr183 to Phe183 resulted in 70% loss of polymerase activity and a significant increase in the fidelity of DNA synthesis. Based on our results and molecular modeling studies, we predicted that the side chain of Y183 is stabilized via its interaction with the side chain of Gln91 (47). This interaction was indeed observed in a subsequently solved 3-D crystal structure of RT-DNA-dNTP ternary complex where van der Waals interaction between the side chain of Q91 and Y183 was noted (10). We hypothesized that the loss of polymerase activity by Tyr→Phe substitution may be manifested due to loss of this interaction. Thus, a similar influence on the polymerase function of the enzyme can be expected if this interaction between Y183 and Q91 is perturbed by mutation at position 91. As per our hypothesis, removal or reduction in the length of the side chain at position 91 (Gln→Ala or Gln→Asn) resulted in significant loss of polymerase activity of the enzyme, probably due to loss of its side chain interaction with Tyr183. The same mutants exhibit revival of polymerase activity when a mutation with valine is introduced at the 184 position. These results have been discussed in the context of the 3-D crystal structure of HIV-1 RT-DNA-dNTP ternary complex (10).

MATERIALS AND METHODS

The mutagen-M13 *in-vitro* mutagenesis kit was obtained from Bio-Rad laboratories. The Sequenase and DNA sequencing reagents were from U.S. Biochemicals. Restriction endonucleases, DNA-modifying enzymes, and HPLC-purified dNTPs were from Boehringer Mannheim or Promega; IDA-Sepharose for immobilized metal affinity chromatography (IMAC) was purchased from Pharmacia; ^{32}P-labeled dNTPs and ATP were obtained from PerkinElmer. Synthetic template-primers, sequencing primers, and mutagenic oligonucleotides were synthesized at the Molecular Resource Facility at UMDNJ. An HIV-1 RNA expression clone, *p*HIV-PBS, was a generous gift from Dr. M. A. Wainberg (48). All other reagents were of the highest available purity grade and were purchased from Fisher, Millipore, Boehringer Mannheim, and Bio-Rad.

Expression Plasmid Clones and In-Vitro Mutagenesis

Two recombinant plasmids, pKK-RT66 and pET-28a-RT51, containing P66 and P51 encoding regions, were used for isolating wild-type heterodimeric HIV-1 RT (29). The smaller subunit contained His-tag sequences at the N-terminal region. The *EcoRI* and *Kpn1* fragment (1.432 kb) of pKK-RT66 encoding the polymerase domain of HIV-1 RT was subcloned in bacteriophage M13 mp18 and used as the template for site-directed mutagenesis. The mutagenesis protocol using dU- containing DNA template was essentially as described by Kunkel et al. (49). After ascertaining the mutation in M13 by DNA sequencing, the desired mutation was introduced in both the subunits as follows: The *EcoRI* and *Kpn1* fragment from M13 mp18 was cloned in RT66 expression cassette and the *Bal1* and *Kpn1* fragment was cloned in RT51 expression cassette.

Polymerase Activity Assay

An HIV-RNA expression clone (pHIV-PBS) was used for the preparation of U5-PBS HIV-1 genomic RNA template as described earlier (50). Polymerase activity of the WT and mutant enzymes was assayed on U5-PBS HIV-1 RNA and 49 mer U5-PBS DNA templates primed with 17-mer PBS primer. Assays were done in a 50 μL volume containing 50 mM Tris-HCl (pH 8.0), 100 μg/mL bovine serum albumin, 5 mM MgCl2, 1 mM dithiothreitol, 50 mM KCl, 100 nM TP, and 100 μM dNTP (25 μM of each of the four dNTPs) with one of them being labeled with ^{32}P (0.2 μCi/nmol dNTP) and 10 nM enzyme. Reactions, carried out at 37°C for 5 min, were terminated by the addition of ice-cold 5% trichloroacetic acid containing 5 mM inorganic pyrophosphate. The samples were filtered on Whatman GF/B filters and processed for radioactivity counting as described before (51).

Steady-State Kinetics of Polymerization

The kinetic studies were carried out at 25°C as described before (26) using homopolymeric poly rA.dT_{18} and poly rC.dG_{18} as the template primers and corresponding complementary dTTP and dGTP as the substrates. Template primer was prepared by mixing equimolar amounts of template and primer at 20 μM concentrations. The reaction mixture contained 50 mM Tris-HCl, pH 7.5, 2 mM MgCl2, 1 mM DTT, 100 μg of BSA/mL, 100 nM of template-primer and varying concentration of [^{3}H]-dTTP substrate. The specific radioactivity of [^{3}H]-dTTP substrate (CPM/pmol) was adjusted by the addition of unlabeled dTTP. The concentration of enzyme used in the assay ranged from 20 nM for the wild-type enzyme to 40 nM for the mutants. The reaction was initiated by the addition of $MgCl_2$ and terminated by the addition of 5% ice-cold TCA at desired time points. The TCA-precipitable materials were collected on Whatman GF/B filters and counted for radioactivity in liquid scintillation counter. The kinetic constants for the polymerase reaction catalyzed by the wild-type HIV-1 RT and its mutant derivatives were determined graphically by Eadie-Hofstee plots of the initial velocity data, using the program Enzyme Kinetics v1.1. The $k_{cat}(s^{-1})$ were calculated from the equation $V_{max}=k_{cat} \times [E]$.

Gel analysis of polymerase reaction products

For the gel analysis, 5′-^{32}P-labeled PBS DNA primer annealed with U5-PBS HIV-1 RNA or 49-mer U5-PBS DNA template was used in the polymerase reaction as described above. The primers were end-labeled with ^{32}P using T4 polynucleotide kinase and [γ-^{32}P] ATP (3,000 Ci/mmol) according to the standard protocol (52). The reaction mixture contained 50 mM Tris-HCl (pH 8.0), 100 μg/mL bovine serum albumin, 5 mM $MgCl_2$,1 mM DTT, 50 mM KCl, 100 nM TP, 100 μM dNTP (25 μM of each of the four dNTPs), and 10 nM enzyme in a total volume of 6 μL. The reactions were terminated by the addition of 6 μL of Sanger's gel loading dye (53) containing 20 mM EDTA. The extension products were resolved on a 10% denaturing polyacrylamide-urea sequencing gel.

ddNTP sensitivity assay

The template primers used in this assay included the U5-PBS RNA primed with ^{32}P -labeled 17-mer DNA primer. Samples were incubated at 37°C for 5 min prior to termination using an equal volume of Sanger's dye as described before. Final concentrations of dNTP were 10 μM; those of ddNTP were 5 μM each. All other conditions were similar to the polymerase assay.

Determination of inhibitor constants (Ki) and *half-maximal inhibitory constant* (IC_{50}) for dideoxy nucleotide inhibitors

The wild type HIV-1 RT and mutant derivatives were examined for their ability to incorporate ddTTP and ddGTP using the poly rA.dT_{18} and poly rC-dG_{18} as the template-

primers and complementary dTTP and dGTP as the substrates, respectively. Three independent experiments were carried out using variable concentrations of ddNTP inhibitor while keeping the concentrations of dNTP (10 μM) and template primer (100 nM) constant. The radioactive label was [^{3}H] labeled dTTP or dGTP (1μCi/per assay). The enzymes (10 nM) were preincubated with the template primer for 2 min at 25 °C prior to initiation of DNA synthesis by addition of a mixture of magnesium complex of dTTP and ddTTP. The reactions were carried out for 3 min at 37 °C in a standard reaction mixture in 50 μL and were terminated by the addition of cold 5% TCA containing 5 mM PPi. The reaction mixtures were then filtered on Whatman GF/B filters to wash away all free dTTP, and the filters were dried and counted in a liquid scintillation counter. The Ki value of ddNTP was determined from percent inhibition using the equation (a) and IC_{50} values were determined using the equation (b) for the competitive inhibitor (54).

$$\%i=\frac{[I]\,100}{Ki\,(1+\frac{[S]}{K_m})+[I]} \quad \text{(a)}$$

$$IC_{50}=Ki\,(1+\frac{[S]}{K_m}) \quad \text{(b)}$$

rNTP incorporation assay

The ability of the wild-type and its mutant derivatives to incorporate rNTPs as substrate was assayed on both RNA and DNA templates. The U5-PBS RNA template and 49-mer U5-PBS DNA primed with ^{32}P labeled 17-mer DNA were used as RNA-DNA and DNA-DNA TP. In each case, enzyme was preincubated with labeled TP. Reactions were initiated by addition of dNTP (200 μM) or rNTP (500 μM). The reactions were done in a total volume of 6 μL and terminated by adding loading dye as described before. The terminated reaction products were heated to 90°C and resolved on an 8% denaturing polyacrylamide gel (8M urea, 1X TBE) sequencing gel.

Extension of primers in the presence of three dNTPs

5′-^{32}P-labeled 17-mer primer annealed with a three-fold excess of 49-mer U5-PBS DNA or U5-PBS primer RNA was used to determine the extent of misincorporation in the presence of only three dNTPs. The labeled template primer was incubated with 10 nM WT or mutant enzymes at 37°C for 10 min in a total volume of 6 μL containing) mM Tris-HCl (pH 7.5), 1mM DTT, 0.1 mg of BSA per mL, 5 mM $MgCl_2$ and only three dNTPs at a concentration of 200 μM each (-A= dCTP, dGTP, dTTP; -G= dATP, dCTP, dTTP; -C = dATP, dGTP, dTTP; -T= dATP, dCTP, dGTP). At the end of incubation the reaction was quenched by adding 6 μL of Sanger's gel loading dye. The reaction products were analyzed on a denaturing 10% polyacrylamide (8M urea) gel.

Measurement of pyrophosphorolysis reaction

Pyrophosphorolysis activity of the mutant enzymes was estimated by analyzing the products of the reaction on denaturing polyacrylamide gels. U5-PBS HIV-1 RNA and 49-mer U5-PBS DNA templates primed with ^{32}P-labeled 17-mer PBS primers were used for measurement of the pyrophosphorolysis reaction. The 6 μL reaction mixture contained 50 mM Tris-HCl (pH 7.5), 1mM DTT, 100 μg BSA, 5 mM $MgCl_2$, 1 mM sodium pyrophosphate, and 10 nM enzyme. The reactions were done for 30 min and quenched by adding an equal volume of Sanger's gel loading dye. The samples were then heated at 95°C

and loaded on denaturing 12% polyacrylamide-8M urea gel. The labeled products were detected by autoradiography.

Molecular Modeling—The coordinates of 3D structure of HIV-1 RT in E-TP-dNTP ternary complex were taken from the RCSB PDB 1RTD file (10). To analyze the interaction of mutant derivatives of Q91 and M184, the crystal structure of RT was altered to include the respective amino acid substitutions. Mutations were introduced using Maestro v8.0 (Schrodinger, L.L.C., New York). Structure display was done using the Maestro graphical interface. The wild-type and mutant enzyme complexes were energy-minimized according to a protein refinement protocol implemented in Macromodel v9.5 (Schrodinger LLC, New York), using the OPLS-AA force-field parameters. The resulting models were used to interpret the observed biochemical properties of the mutant derivatives in context of wild-type enzyme structure.

RESULTS

Construction and purification of mutant enzymes

Two mutant derivatives of residue position 91 and two double mutants at positions 91 and 184 of HIV-1 RT were constructed and expressed in *E. coli* by the procedure described before (47). Two single substitutions were carried out in which the functional side chain of Gln91 was abolished, in one case by replacing it with Ala and in the other by replacing with conservative Asn residue, which displays geometry and polarity in its side chain that is similar to that of Gln. The double mutants at positions 91 and 184 were Q91N/M184V and Q91A/M184V. The purified enzyme preparations were found to be homogeneous with a purity of greater than 95%. The level of their expressions, solubility, yield and heat inactivation pattern of all the mutant proteins, were identical to that of the wild-type enzyme, indicating that these mutation had not altered the folded structure of the enzyme protein.

Polymerase activity of the wild type and its mutant derivatives on RNA and DNA templates

Various mutations of HIV-1 RT have displayed differential polymerase activity with different template primers. Earlier, we demonstrated that alanine substitution at positions 72 and 151 results in impairment of the polymerase activity by nearly an order of magnitude with RNA template, while only a 5-fold reduction was seen with DNA-directed reactions (22,27). To determine whether the mutant derivatives of Gln91 share this template preference, we evaluated their polymerase activity with different template primers.

Polymerase activities of the wild-type HIV-1 RT and its mutant derivatives were assessed using poly (rA).$(dT)_{18}$ as well as natural RNA and DNA templates corresponding to the U5-PBS region of HIV-1 genome primed with a PBS primer. The results shown in Table 1 indicate that polymerase activity of Q91A mutant is only 8–12% of the WT activity on both the heteromeric and homopolymeric TP whereas Q91N retained 30% activity with the heteromeric U5-PBS TP while 56% activity was observed with the homopolymeric poly rA/dT TP. The polymerase activity of double mutants Q91A/M184V and Q91N/184V was significantly improved on both the template primers. The gel extension assays showed similar activity pattern for single and double mutant enzymes. The results (Fig. 1) indicate that both Q91A and Q91N mutant enzymes are severely impaired in their polymerase activity in relation to the wild-type enzyme on both RNA and DNA templates. Polymerase activity of the Q91A seems to be severely impaired, leaving the enzyme almost defective; Q91N mutant enzyme also shows much less activity. Interestingly, the extent of primer extension exhibited by Q91N mutant was greatly reduced as compared to the wild-type enzyme. Q91N mutant seems to pause more frequently and accumulate shorter products,

although the degree of initial primer use is similar to that by the wild-type enzyme. Notably, the observed "pausing" pattern of Q91N mutant enzyme is similar on both RNA and DNA templates. Most interestingly, the deleterious effect of the mutation was reduced when the M184V mutation was introduced in addition to Q91A, while the Q91N/M184V mutant showed activity similar to that of the wild-type enzyme. Thus it is possible that the decreased polymerase activity of both Q91A and Q91N may be due to subtle changes in the dNTP binding pocket. Such a change in the pocket may also influence the fidelity and processivity of the enzyme, as well as its response to ddNTP inhibitors.

Steady-State Kinetics Analysis

The kinetic parameters of the mutant derivatives of Q91 determined using homopolymeric poly-rA.dT_{18} and poly-rC.dG_{18} templates indicated a drastic reduction in the utilization of substrate (higher K_{mdTTP}) by both Q91A and its double mutant derivative Q91A/M184V while Q91N and its double mutant derivative, Q91N/M184V displayed K_{mdTTP} similar to the wild type enzyme A 10–12 fold increase in *K*m for dTTP for the Q91A and Q91A/M184V mutants on the homopolymeric poly-rA.dT_{18} template was noted with corresponding 21- and 43-fold decrease in the catalytic efficiency, respectively (Table 2). Similar 5–10 fold increase in K_{mdGTP} for Q91A and Q91A/M184V mutants was noted on homopolymeric poly-rC.dG_{18} template with corresponding 27–32 fold decrease in the catalytic efficiency. In contrast, the Q91N and Q91N/M184V double mutant showed no significant change in their K_m value for dGTP substrate with 2–3 fold decrease in their catalytic efficiency on poly rA template and 5–10 fold decrease on poly rC template. As expected, M184V mutant displayed kinetic behavior similar to the wild type enzyme. These kinetic parameters confirms that Ala substitution at position 91 severely impair the dNTP binding and polymerase function of the enzyme. These results confirm our earlier postulation that Q91 may be involved in stabilizing the side chain of Tyr at position Y183; an important residue in the YMDD motif and a constituent of dNTP binding pocket. A significant loss of polymerase activity was also observed by a conservative substitution from Glu to Asn at this position without any significant change in the substrate utilization. Although shorter side chain of conservative Asn may still interact with Tyr 183 to stabilize the dNTP pocket, it may compromise the flexibility of the pocket that may result in increase in the fidelity and reduced sensitivity to dideoxy nucleotide analog.

Sensitivity of WT HIV-1 RT and mutant derivatives to ddNTPs

Dideoxy ribonucleotides have been shown to be competitive inhibitors of HIV-1 RT and have also been used to treat AIDS. The most potent single-agent nucleoside among the approved nucleoside inhibitors is (−)-β-2′, 3′-dideoxy-3′-thiacytidine (3TC, Lamivudine). However, in both cell culture and patients, resistance to 3TC develops rapidly. Resistant variants containing an M184I alteration in RT gene appear transiently and then are replaced by those with M184V alteration (55). This M184V mutation has also been shown to confer low-level resistance on ddI and ddC (35). An E89G substitution reportedly confers multiple resistances to ddNTPs in cell-free analysis (32). This mutation also confers resistance on nonnucleoside RT inhibitors and foscarnet, a PPi analog, both *in vivo* and *in vitro* (32). We have shown that substitution at position 183 confers resistance on ddNTPs *in vitro* (47). Since Y183 and Q91 have been proposed to stabilize each other via hydrogen bonding interaction, it was interesting to examine the influence of Q91 substitution on the ddNTP sensitivity of the mutant enzymes compared to the wild-type enzyme. As shown in Figure 2, both mutations vary in their ability to change response of RT to ddNTP analogs. In the case of Q91N, comparison of the lane representing synthesis in the absence of ddNTP (Fig. 1) and in the presence of ddATP, ddCTP, ddGTP, and ddTTP (Fig. 2) indicates that Q91N substitution confers higher resistance on the ddNTP analogs. These results suggest that the substitution has affected the enzyme activity in a manner similar to that affected by E89G or

Y183F alteration. While Q91A/M184V double mutant also shows resistance to ddNTPs, Q91N/M184V double mutant shows sensitivity similar to the wild-type enzyme. The Ki) and IC_{50} of ddTTP and ddGTP determined with mutant derivatives carrying single and double mutants shows similar patterns as seen in the gel extension assay (Table 3). As expected both Q91A and Q91N displayed higher Ki and IC_{50} values as compared to M184V and the wild type enzyme. A second substitution at position 184 (M184V) improved the affinity for these analogs with lower Ki and IC_{50} values as compared to the single mutants. The M184V mutant higher Ki values for ddTTP and ddGTP as compared to the wild type enzyme but lower than the single and double mutants.

Fidelity of the wild-type and mutant enzymes

Several previous studies have suggested that nucleoside analog resistance may be associated with increased fidelity of HIV-1 RT. Mutant enzymes such as M184V (29, 30), E89G (35, 56), and M184L (57) have been shown to exhibit higher enzyme fidelity than does the wild-type enzyme. On the other hand, alterations such as Asn67 and Arg70 have been shown to exhibit high levels of resistance to nucleoside analogs but decreased enzyme fidelity (58, 59). Hence, ddNTP resistance and fidelity of the enzyme seem to be closely related and to affect each other. Thus it was interesting to examine whether Q91A and Q91N mutations, either separately or in the presence of double mutation M184V, influence these functions of the enzyme. The assay used here measures the net result of both misinsertion and subsequent mispair extension by omitting a single dNTP from the polymerization reaction. Results, shown in Figure 3, suggest an overall increase in fidelity for both of the mutant enzymes as compared to the wild-type enzyme. Of the two mutant enzymes, Q91N mutant enzyme seems to be more discriminatory than is the WT enzyme. As compared to the wild-type as well as the Q91A/M184V and Q91N/M184V mutants, Q91N mutant seems to be more discriminatory for incorporation of dNTP, as well as the extension of primers, once a misinsertion has taken place.

All these studies suggest the likelihood that both resistance to nucleoside analogs and increase in fidelity involve similar mechanisms whereby the ability to incorporate or reject an incoming dNTP or its analog is accompanied by the ability to recognize the right dNTP for insertion. One might imagine that such high-fidelity enzymes might be advantageous for survival of the virus under the selection pressure of a drug, since the enzyme will be less error-prone.

Incorporation of rNTP versus dNTP

The high discrimination that mutant enzymes exhibited with respect to the incorporation of ddNTP or incorrect dNTP prompted us to study the ability of the enzymes to discriminate between rNTP and dNTP. To assay the ability of mutant enzymes to discriminate between rNTP and dNTP, incorporation of both was studied on primed U5-PBS RNA and U5-PBS DNA templates as described. As shown in Figure 4, none of the mutant RT derivatives have incorporated rNTPs as much as seen by wild-type RT, although extent of rNTP incorporation by Q91N/M184V mutant derivative was similar to the wild type enzyme. The Q91N mutant derivative of RT seems to be more discriminatory than are the Q91A/M184V and Q91N/M184V double mutant derivatives for both the DNA and RNA templates. If use of rNTP as compared to that of dNTP can be taken as a function of enzyme fidelity, then this result supports our earlier observation that Q91N exhibits increased fidelity.

Pyrophosphorolysis

This process is the reversal of polymerase activity resulting in cleavage of the DNA primer from the 3′ terminus in the presence of PPi. It results in the generation of dNTPs as the products. Pyrophosphorolysis could be extremely important for survival of HIV -1 under the

pressure of drug therapy *in vivo* in order to remove chain-terminating 3′-deoxynucleosides, thereby allowing additional chain elongation. Arion *et al.* (58) *have reported* such enhanced pyrophosphorolysis in HIV-1 RT due to mutations D76N/K70R in the high-level resistance mutants D76N, K70R, T215F, and K219Q. We have reported that mutations in the residues from the dNTP binding pocket changed the pyrophosphorolysis activity of the enzyme in a template-dependent manner (21). It is possible that the observed resistance to ddNTP of Q91A and Q91N mutant enzymes could be due to increased pyrophosphorolysis activity, which can generate 3′-OH by cleaving the ddNTP-terminated primer. To examine this possibility, the pyrophosphorolysis activity of these mutant enzymes was studied. Of the four mutant derivatives studied in this work, Q91N/M184V, independent of the template used, was comparable to wild-type enzyme in its pyrophosphorolysis activity. As depicted in Figure 5, Q91A, Q91N, and Q91A/M184V derivatives were much less efficient in the catalysis of pyrophosphorolysis activity on both DNA and RNA templates. It should be noted that both of the mutant derivatives are deficient in their polymerase activity. Arion *et al.* (58) have reported a concomitant increase in the processivity of the mutant enzyme D76N, K70R, T215F, and K219Q to compensate for the increased pyrophosphorolysis, which they attribute to alterations T215F and K219Q. Similarly, Conrad *et al.* (59) have proposed that an RT enzyme containing the AZT resistant mutation can selectively remove an AZT-MP-terminated primer-template due to enhanced pyrophosphorolysis.

DISCUSSION

In the 3D crystal structure of HIV-1 RT, Gln91 is located on the β5a-β5b loop of the palm subdomain in the polymerase cleft (8). Our previous studies, have suggested the involvement of residue at position 91 through its interaction with the side chain of Y183, a constituent of the highly conserved YXDD motif found in all retroviral reverse transcriptases (47). Analyses of 3D crystal structure-based molecular model of ternary complex have indicated that the side chains of Q91 and Y83 are in close proximity and may stabilize each other through hydrogen bonding interaction (47). This prediction was nearly validated with availability of the 3D crystal structure of HIV-1 RT-DNA-dNTP ternary complex, in which the hydroxyl group of Y183 and the side chain amide group of Q91 are positioned at a distance appropriate for van der Waals interaction. However, it is possible that the dynamic structure of ternary complex of HIV-1 RT in solution may also assume side chain conformations of Q91 and Y183 to favor hydrogen bonding interaction between them. The systematic search for side chain conformation of both Q91 and Y183 does indicate the existence of such conformations appropriate for hydrogen bonding. Abolishment of this interaction by substitution of Tyr→Phe at position 183 resulted in 70% loss of polymerase activity on both the RNA and DNA templates, with a significant increase in the fidelity. It was expected that similar mutations at position 91 might also manifest enzyme characteristics similar to those observed for Y183F mutant. In the present study we examined the biochemical properties of mutant derivatives of Q91 with wild type background at position 183. Since deleterious effect of Y183F mutation was reversed by introducing a second M184V mutation (47), we proposed to examine if similar reversal effect could be seen on Q91 mutants by introducing M→V mutation at 184 position with wild type side chain at position 183.

To elucidate the possible role of residue 91 in HIV-1 RT, two mutations were introduced at position 91 and one mutation at position 184, replacing Me→Val in addition to the 91 mutation. Mutant enzymes Q91A, carrying a nonconservative substitution, and Q91N, with a conservative substitution, were studied. As predicted, both substitutions severely affected the polymerase activity of the enzyme. Q91A mutant enzyme was found to be more impaired in its polymerase activity than was the Q91N mutant enzyme. However, when another mutation was introduced at position 184, it seemed to compensate for the deleterious

effect of the 91 mutation. The compensating effect was more pronounced when the 184 mutation was in the presence of the Q91N mutation. Moreover, the double mutant showed activity comparable to that of wild-type enzyme. Such results have been previously described for mutations involving residues in the dNTP binding pocket (21). These observations suggest that the decreased polymerase activity could be due to the indirect effect of these mutations on dNTP binding. Our study of sensitivity of the mutant enzymes to the ddNTP analogs has shown that both the enzymes are more resistant than is the wild-type enzyme to all the ddNTPs, but to a variable degree. The Q91N enzyme seems to be more resistant to ddNTPs than is Q91A/M184V and Q91N/M184V mutant enzymes as judged by gel extension assay and higher Ki and IC_{50} values for these analogs. In general, Q91N enzyme presents a pattern of resistance to ddNTPs similar to that of the Y183F mutant enzyme (47). Enzyme fidelity, as studied by the polymerase reaction in the absence of one dNTP, suggests higher enzyme fidelity for Q91N substitution in relation to wild-type and both Q91A/M184V and Q91N/M184V mutant enzymes on DNA and RNA templates. The observation that Q91N also has more discriminatory ability is further supported by our results regarding use of rNTP against dNTP for all four mutant enzymes.

Interestingly, the results for mutant Q91N clearly suggest that this mutant behaves somewhat similarly to Y183F mutant derivative of HIV-1 RT. We have earlier predicted that side chain of Q91 may be involved in the stabilization of the side chain of Y183 (47). The same results also point toward the possible involvement of residue at position 91 in the pyrophosphorolysis activity of HIV-1 RT. We have also noted that the Y183F mutant RT was severely impaired in its catalysis of pyrophosphorolysis on a DNA template. To summarize, Q91N/M184V double mutant was found to be similar to the wild-type enzyme with respect to its ddNTP sensitivity, rNTP utilization and fidelity, whereas Q91A/M184V double mutant is much less efficient than the wild-type enzyme. Q91N mutant derivative is characterized by increased resistance to ddNTP analogs and increased fidelity.

These enzyme characteristics are similar to those of the E89G mutant enzyme that has been isolated from HIV-1 infected cell culture (32). However, the E89G mutant enzyme has been shown to have higher processivity, which probably compensates for its decreased forward synthesis, a consequence of decreased polymerase activity and increased fidelity (65). An enzyme with increased pyrophosphorolysis as compared to its polymerase activity and decreased processivity could be detrimental to viral replication *in vivo*. Increased fidelity tends to slow the forward reaction further. We expect that it may be difficult for such a mutation to survive *in vivo*. Indeed, mutation at this position has not so far been reported in HIV-1 variants isolated from AIDS patients or from HIV-1 infected cell cultures. Moreover, this supposition has been supported by studies of Tachedjian *et al.* (61). *While examining the inverse nature of interaction between AZT resistant and foscarnet (phosphonoformic acid, PFA)-resistant mutants in vivo, they intended to introduce PFA resistance, one involving residue 89 (E89K) into engineered AZT resistant background. Their attempts to recover infectious viruses containing mutation Q91L were not successful and they concluded that this mutation might not be viable. Interestingly, the same authors readily isolated E89K as a PFA-resistant mutation from MT-2 cells exposed to increasing concentrations of the drug. This drug is a PPi analog used to treat infections due to cytomegalovirus (such as retinitis) in AIDS patients. In a study that compared PFA with ganciclovir for treatment of CMV retinitis in AIDS patients* (62, 63), the antiretroviral effect of PFA was suggested as one possible explanation of the improved survival of PFA-treated patients. It has been reported that mutation E89G is resistant to PFA, along with ddTTP, ddCTP, ddATP, ddGTP, AZTTP, and 3TCTP. This resistance and the increased processivity of E89 have been attributed to its interaction with the penultimate nucleotide of the double-stranded template (35).

All of these results point toward the possible involvement of residues 89 and 91 in the pyrophosphorolysis activity of HIV-1 RT, probably via their interaction with the template primer duplex. Any catalytically important residue for an enzyme activity is expected to be fairly well conserved in sequences carrying out similar functions in nature. Xiong and Eichenbush (63), in studies of the origin and evolution of retro-elements based on their reverse transcriptase sequences, have noted that Q at position 91 has been conserved in 17 of 29 retroviral sequences, or more than 60% including in the related viruses HIV-1, HIV-2, and SIV (65). In the rest of the retroviral sequences reported, it is either serine (5 out of 29) or valine (6 out of 29), while in case of human spuma retrovirus, it is asparagine. Interestingly, although the neighboring residues of 91 have been implicated in drug resistance, there have been no reports of the involvement of 91 in any functional aspects of HIV-1 RT. The absence of reports on involvement of residue 91 in drug resistance might indirectly imply that mutation at this position is not viable. This postulation is supported by the studies of Tachedjian *et al. (66*), in which HIV-1 carrying a Q91L mutation in the RT gene was found to be noninfectious and replication-incompetent.

In a 3D crystal structure of the RT-DNA-dNTP ternary complex (10), a residue at position 91 is within interacting distance from the side chains of Tyr183 and Gln161, as well as the penultimate base of the primer. To analyze the inter-residue and residue-primer interactions, we did mutant modeling of Q91A and Q91N, as well as double mutants Q91A/M184V and Q91N/M184V in the 3D crystal structure of the ternary complex (10). As shown in Figure 6A, the side chain hydroxyl group of Y183 is located near the primer terminus in such a way that it forms hydrogen bonding interaction with the penultimate base of the primer (Y183 -OH---N_3 primer base); it is also located at 3.5 Å distance from the amide group of Q91 (Q91 –$CONH_2$---OH Y183) establishing van der Waals interaction. This indicates that the side chain amide group of Q91 has a critical function in stabilizing the primer terminus region though its interaction with Y183. It has been well established that residues interacting with the primer terminus significantly influence the geometry of the dNTP binding pocket. Moreover, point mutations at these positions are implicated in a detrimental effect on polymerase efficiency of the enzyme. Due to the lack of an amide side chain in Q91A, favorable electrostatic interactions do not takes place with the primer terminus and Y183 residue (Fig. 6B). Although the conservative mutant derivative Q91N has an amide side chain like Q91, it is shorter and, as a result, does not form productive interaction with the side chain of Y183 (Fig. 6B). Double mutants Q91A/M184V and Q91N/M184V (Fig. 6C) were able to restore the enzyme activity to a level comparable to that of wild-type enzyme, suggesting that valine, at position 184, has a compensatory role. As shown in Fig. 6A, the side chain of the M184 residue is in close proximity to the primer terminus (M184 β-carbon-primer sugar oxygen atom, 4.8 Å; M184 β-carbon-dTTP sugar oxygen atom, 4.9 Å). The compensatory effect of the M184V mutation on the polymerase activities of both Q91A and Q91N mutant derivatives (Fig. 6C) could be due to stronger interaction of the β-branched valine residue at the 184 position with the primer terminus sugar moiety, as well as the incoming dNTP sugar ring (V184 β-CH_3----primer sugar oxygen atom, 4.3 Å; V184 β-CH_3--dTTP sugar oxygen atom, 4.3 Å). Restoration of the polymerase activity of Q91N/M184V double mutant to the level of wild-type polymerase activity can also be explained based on the closer proximity of Q91N side chain amide group to the Q161 side chain amide group compared to corresponding distance seen in Q91N single mutant (single mutant, Q91N amide ---Q161 amide 3.4 Å versus double mutant, Q91N amide---Q161 amide, 3.0 Å) (Fig. 6B and 6C, respectively). These studies confirm our earlier postulation that side chain of Q91 is essential to stabilize the side chain of Y183, an important constituent of the YMDD motif in HIV-1 RT. Disruption of this interaction by mutation at either of the positions results in similar effect on the fidelity and ddNTP sensitivity and polymerase function of the enzyme. Ding et al have suggested that Y183 might play an important role in positioning the active site of the enzyme during the translocation process following the

catalytic step (67). It can be postulated that in the dynamic structure of HIV-1RT in the solution form, Y183 may display alternating van der Waals and hydrogen bonding interaction with the side chain of Q91. In the ternary complex, it may have van der Waals interaction with Q91 and hydrogen bonding interaction with the second primer nucleotide. During the translocation, the hydrogen bonding of Y183 with the penultimate primer nucleotide would be broken. During this process the side chain of Y183 may reorient and transiently gets stabilized by hydrogen bonding and/or van der Waals interaction with the side chain of Q91 before it reestablishes the hydrogen bonding with the new penultimate primer nucleotide.

Acknowledgments

This research was partly supported by a grant from the NIH/NIAID (AI074477)

Abbreviations used

A, Q, M, N and Y	represent single letter codes for Ala, Gln, Met, Asn and Tyr amino acids, respectively
SDS-PAGE	sodium dodecyl sulfate polyacrylamide gel electrophoresis
DTT	dithiothreitol
Poly (rA). (dT)18	polyriboadenylic acid annealed with (oligodeoxythymidylic acid)18
dNTP	deoxyribonucleoside triphosphate
dATP, dGTP, dCTP and dTTP	represent nucleoside triphosphate of deoxyadenosine, deoxyguanosine, deoxycytidine and thymidine, respectively
HIV-1 RT	human immunodeficiency virus type 1 reverse transcriptase
IMAC	immobilized metal affinity chromatography
IDA-Sepharose	iminodiacetic acid-Sepharose
U5-PBS RNA template	HIV-1 genomic RNA template corresponding to primer binding sequence region
U5-PBS DNA template	DNA template corresponding to the U5-PBS HIV-1 genomic RNA sequence

References

1. Wei X, Ghosh SK, Taylor ME, Johnson VA, Emini EA, Deutsch P, Lifson JD, Bonhoeffer S, Novak MA, Hahn BH, Saag MS, Shaw GM. Viral dynamics in human immunodeficiency virus type 1 infection. Nature. 1995; 373:117–122. [PubMed: 7529365]
2. Ho DD, Neumann AU, Perelson AS, Chen W, Leonard JM, Markowitz M. Rapid turnover of plasma virions and CD4 lymphocytes in HIV-1 infection. Nature. 1995; 373:123–126. [PubMed: 7816094]
3. Tuske S, Sarafianos SG, Clark AD Jr, Ding J, Naeger LK, White KL, Miller MD, Gibbs CS, Boyer PL, Clark P, Wang G, Gaffney BL, Jones RA, Jerina DM, Hughes SH, Arnold E. Structures of HIV-1 RT-DNA complexes before and after incorporation of the anti-AIDS drug tenofovir. Nat Struct Mol Biol. 2004; 11:469–474. [PubMed: 15107837]
4. Das K, Bandwar RP, White KL, Feng JY, Sarafianos SG, Tuske S, Tu X, Clark AD Jr, Boyer PL, Hou X, Gaffney BL, Jones RA, Miller MD, Hughes SH, Arnold E. Structural basis for the role of the K65R mutation in HIV-1 reverse transcriptase polymerization, excision antagonism, and tenofovir resistance. J Biol Chem. 2009; 284:35092–35100. [PubMed: 19812032]

5. Esnouf R, Ren J, Ross C, Jones Y, Stammers D, Stuart D. Mechanism of inhibition of HIV-1 reverse transcriptase by non-nucleoside inhibitors. Nat Struct Biol. 1995; 2:303–308. [PubMed: 7540935]
6. Ren J, Esnouf R, Garman E, Somers D, Ross C, Kirby I, Keeling J, Darby G, Jones Y, Stuart D, Stammers D. High resolution structures of HIV-1 RT from four RT–inhibitor complexes. Nat Struc Biol. 1995; 2:293–302.
7. Rodgers DW, Gamblin SJ, Harris BA, Ray S, Culp JS, Hellmig B, Woolf DJ, Debouck C, Harrison SC. The structure of unliganded reverse transcriptase from the human immunodeficiency virus type 1. Proc Natl Acad Sci USA. 1995; 92:1222–1226. [PubMed: 7532306]
8. Kohlstaedt LA, Wang J, Friedman JM, Rice PA, Steitz TA. Crystal structure at 3.5 Å resolution of HIV-1 reverse transcriptase complexed with an inhibitor. Science. 1992; 256:1783–1790. [PubMed: 1377403]
9. Das K, Ding J, Hsiou Y, Clark AD Jr, Moereels H, Koymans L, Andries K, Pauwels R, Janssen PA, Boyer PL, Clark P, Smith RH Jr, Kroeger Smith MB, Michejda CJ, Hughes SH, Arnold E. Crystal structures of 8-Cl and 9-Cl TIBO complexed with wild-type HIV-1 RT and 8-Cl TIBO complexed with the Tyr181Cys HIV-1 RT drug-resistant mutant. J Mol Biol. 1996; 264:1085–1100. [PubMed: 9000632]
10. Huang H, Chopra R, Verdine GL, Harrison SC. Structure of a covalently trapped catalytic complex of HIV-1 reverse transcriptase: implications for drug resistance. Science. 1998; 282:1669–1675. [PubMed: 9831551]
11. Larder BA, Purifoy DJM, Powell KL, Darby G. Site-specific mutagenesis of AIDS virus reverse transcriptase. Nature. 1987; 327:716–717. [PubMed: 2439916]
12. Larder BA, Kemp SD. Multiple mutations in HIV-1 reverse transcriptase confer high-level resistance to zidovudine (AZT). Science. 1989; 246:1155–1158. [PubMed: 2479983]
13. Boyer PL, Ferris AL, Hughes SH. Cassette mutagenesis of the reverse transcriptase of human immunodeficiency virus type 1. J Virol. 1992; 66:1031–1039. [PubMed: 1370546]
14. Boyer PL, Ferris AL, Clark P, Whitmer J, Frank P, Tantillo C, Arnold E, Hughes SH. Mutational analysis of the fingers and palm subdomains of human immunodeficiency virus type-1 (HIV-1) reverse transcriptase. J Mol Biol. 1994; 243:472–483. [PubMed: 7525967]
15. Wilson JE, Aulabaugh A, Caligan B, McPherson S, Wakefield JK, Jablonski S, Morrow CD, Reardon JE, Furman PA. Human immunodeficiency virus type-1 reverse transcriptase. Contribution of Met-184 to binding of nucleoside 5′-triphosphate. J Biol Chem. 1996; 271:13656–13662. [PubMed: 8662909]
16. Chao SF, Chan VL, Juranka P, Kaplan AH, Swanstrom R, Hutchison CA 3rd. Mutational sensitivity patterns define critical residues in the palm subdomain of the reverse transcriptase of human immunodeficiency virus type 1. Nucl Acids Res. 1995; 23:803–810. [PubMed: 7535923]
17. Tisdale M, Kemp SD, Parry NR, Larder BA. Rapid in vitro selection of human immunodeficiency virus type 1 resistant to 3′-thiacytidine inhibitors due to a mutation in the YMDD region of reverse transcriptase. Proc Natl Acad Sci USA. 1993; 90:5653–5356. [PubMed: 7685907]
18. Sarafianos SG, Marchand B, Das K, Himmel DM, Parniak MA, Hughes SH, Arnold E. Structure and function of HIV-1 reverse transcriptase: molecular mechanisms of polymerization and inhibition. J Mol Biol. 2009; 385:693–713. [PubMed: 19022262]
19. Singh K, Marchand B, Kirby KA, Michailidis E, Sarafianos SG. Structural Aspects of Drug Resistance and Inhibition of HIV-1 Reverse Transcriptase. Viruses. 2010; 2:606–638. [PubMed: 20376302]
20. Menéndez-Arias, Luis. Mechanisms of resistance to nucleoside analogue inhibitors of HIV-1 reverse transcriptase. Virus Res. 2008; 134:124–146. [PubMed: 18272247]
21. Harris D, Kaushik N, Pandey PK, Yadav PNS, Pandey VN. Functional Analysis of Amino Acid Residues Constituting the dNTP Binding Pocket of HIV-1 Reverse Transcriptase. J Biol Chem. 1998; 273:33624 – 33634. [PubMed: 9837947]
22. Sarafianos SG, Pandey VN, Kaushik N, Modak MJ. Site-directed Mutagenesis of Arginine 72 of HIV-1 Reverse Transcriptase. J Biol Chem. 1995; 270:19729–19735. [PubMed: 7544345]

23. Sarafianos SG, Pandey VN, Kaushik N, Modak MJ. Glutamine 151 participates in the substrate dNTP binding function of HIV-1 reverse transcriptase. Biochemistry. 1995; 34:7207–7216. [PubMed: 7539293]
24. Shirasaka T, Kavlick MF, Ueno T, Gao WY, Kojima E, Alcaide ML, Chokekijchai S, Roy BM, Arnold E, Yarchoan R, Mitsuya H. Proc Natl Acad Sci USA. 1995; 92:2398–2402. [PubMed: 7534421]
25. Ueno T, Shirasaka T, Mitsuya H. Enzymatic Characterization of Human Immunodeficiency Virus Type 1 Reverse Transcriptase Resistant to Multiple 2′,3′-Dideoxynucleoside 5′-Triphosphates. J Biol Chem. 1995; 270:23605–23611. [PubMed: 7559526]
26. Kaushik N, Rege N, Yadav PNS, Sarafianos SG, Modak MJ, Pandey VN. Biochemical Analysis of Catalytically Crucial Aspartate Mutants of Human Immunodeficiency Virus Type 1 Reverse Transcriptase. Biochemistry. 1996; 35:11536–11546. [PubMed: 8794733]
27. Kaushik N, Harris D, Rege N, Modak MJ, Yadav PNS, Pandey VN. Role of Glutamine-151 of Human Immunodeficiency Virus Type-1 Reverse Transcriptase in RNA-Directed DNA Synthesis. Biochemistry. 1997; 36:14430–14438. [PubMed: 9398161]
28. Kaushik N, Talele TT, Pandey PK, Harris D, Yadav PNS, Pandey VN. Role of Glutamine 151 of Human Immunodeficiency Virus Type-1 Reverse Transcriptase in Substrate Selection As Assessed by Site-Directed Mutagenesis. Biochemistry. 2000; 39:2912–2920. [PubMed: 10715111]
29. Pandey VN, Kaushik N, Rege N, Sarafianos SG, Yadav PNS, Modak MJ. Role of Methionine 184 of Human Immunodeficiency Virus Type-1 Reverse Transcriptase in the Polymerase Function and Fidelity of DNA Synthesis. Biochemistry. 1996; 35:2168–2179. [PubMed: 8652558]
30. Wainberg MA, Drosopoulos WC, Salomon H, Hsu M, Borkow G, Parniak MA, Gu Z, Song Q, Manne J, Islam S, Castriota G, Prasad VR. Enhanced Fidelity of 3TC-Selected Mutant HIV-1 Reverse Transcriptase. Science. 1996; 271:1282–1285. [PubMed: 8638110]
31. Hsu M, Inouye P, Rezende L, Richard N, Li Z, Prasad VR, Wainberg MA. Higher fidelity of RNA-dependent DNA mispair extension by M184V drug-resistant than wild-type reverse transcriptase of human immunodeficiency virus type 1. Nucleic Acids Res. 1997; 25:4532–4536. [PubMed: 9358162]
32. Prasad VR, Lowy I, de los Santos T, Chiang L, Goff SP. Isolation and characterization of a dideoxyguanosine triphosphate-resistant mutant of human immunodeficiency virus reverse transcriptase. Proc Natl Acad Sci USA. 1991; 88:11363–11367. [PubMed: 1722328]
33. Song Q, Yang G, Goff SP, Prasad VR. Mutagenesis of the Glu-89 residue in human immunodeficiency virus type 1 (HIV-1) and HIV-2 reverse transcriptases: effects on nucleoside analog resistance. J Virol. 1992; 66:7568–7571. [PubMed: 1279207]
34. Kew Y, Qingbin S, Prasad VR. Subunit-selective mutagenesis of Glu-89 residue in human immunodeficiency virus reverse transcriptase. Contribution of p66 and p51 subunits to nucleoside analog sensitivity, divalent cation preference, and steady state kinetic properties. J Biol Chem. 1994; 269:15331–15336. [PubMed: 7515055]
35. Drosopoulos WC, Prasad VR. Increased polymerase fidelity of E89G, a nucleoside analog-resistant variant of human immunodeficiency virus type 1 reverse transcriptase. J Virol. 1996; 70:4834–4838. [PubMed: 8676518]
36. Drosopoulos WC, Prasad VR. Increased Misincorporation Fidelity Observed for Nucleoside Analog Resistance Mutations M184V and E89G in Human Immunodeficiency Virus Type 1 Reverse Transcriptase Does Not Correlate with the Overall Error Rate Measured In Vitro. J Virol. 1998; 72:4224–4230. [PubMed: 9557711]
37. Gutierrez-Rivas M, Ibanez A, Martinez MA, Domingo E, Menendez-Arias L. Mutational analysis of Phe160 within the “palm” subdomain of human immunodeficiency virus type 1 reverse transcriptase. J Mol Biol. 1999; 290:615 –625. [PubMed: 10395818]
38. Jacques PS, Wohrl BM, Ottmann M, Darlix JL, Le Grice SFJ. Mutating the “primer grip” of p66 HIV-1 reverse transcriptase implicates tryptophan-229 in template-primer utilization. J Biol Chem. 1994; 269:26472–26478. [PubMed: 7523408]
39. Palaniappan C, Wisniewski M, Jacques PS, Le Grice SFJ, Fay PJ, Bambara RA. Mutations within the Primer Grip Region of HIV-1 Reverse Transcriptase Result in Loss of RNase H Function. J Biol Chem. 1997; 272:11157–11164. [PubMed: 9111014]

40. Powell MD, Ghosh M, Jacques PS, Howard KJ, LeGrice SFJ, Levin JG. Alanine-scanning Mutations in the “Primer Grip” of p66 HIV-1 Reverse Transcriptase Result in Selective Loss of RNA Priming Activity. J Biol Chem. 1997; 272:13262–13269. [PubMed: 9148945]
41. Ghosh M, Williams J, Powell MD, Levin JG, LeGrice SFJ. Mutating a Conserved Motif of the HIV-1 Reverse Transcriptase Palm Subdomain Alters Primer Utilization. Biochemistry. 1997; 36:5758–5768. [PubMed: 9153416]
42. Ghosh M, Jacques PS, Rodgers DW, Ottman M, Darlix J, Le Grice SFJ. Alterations to the Primer Grip of p66 HIV-1 Reverse Transcriptase and Their Consequences for Template-Primer Utilization. Biochemistry. 1996; 35:8553–8562. [PubMed: 8679616]
43. Yu Q, Ottmann M, Pechoux C, Le Grice SFJ, Darlix J. Mutations in the Primer Grip of Human Immunodeficiency Virus Type 1 Reverse Transcriptase Impair Proviral DNA Synthesis and Virion Maturation. J Viro. 1998; 72:7676–7680.
44. Beard WA, Stahl SJ, Kim HR, Bebenek K, Kumar A, Strub MP, Becerra SP, Kunkel TA, Wilson SH. Structure/function studies of human immunodeficiency virus type 1 reverse transcriptase. Alanine scanning mutagenesis of an alpha-helix in the thumb subdomain. J Biol Chem. 1994; 269:28091–28097. [PubMed: 7525566]
45. Bebenek K, Beard WA, Casas-Finet JR, Kim HR, Darden TA, Wilson SH, Kunkel TA. Reduced Frame shift Fidelity and Processivity of HIV-1 Reverse Transcriptase Mutants Containing Alanine Substitutions in Helix H of the Thumb Subdomain. J Biol Chem. 1995; 270:19516–19523. [PubMed: 7543900]
46. Wilson JE, Aulabaugh A, Caligan B, McPherson S, Wakefield JK, Jablonski S, Morrow CD, Reardon JE, Furman PA. Human Immunodeficiency Virus Type-1 Reverse Transcriptase. J Biol Chem. 1996; 271:13656–13662. [PubMed: 8662909]
47. Harris D, Yadav PNS, Pandey VN. Loss of polymerase activity due to Tyr to Phe substitution in the YMDD motif of human immunodeficiency virus type-1 reverse transcriptase is compensated by Met to Val substitution within the same motif. Biochemistry. 1998; 37:9630–9640. [PubMed: 9657675]
48. Arts EJ, Li X, Gu Z, Kleiman L, Parniak MA, Wainberg MA. Comparison of deoxyoligonucleotide and tRNA(Lys-3) as primers in an endogenous human immunodeficiency virus-1 in vitro reverse transcription/template-switching reaction. J Biol Chem. 1994; 269:14672–14680. [PubMed: 7514178]
49. Kunkel TA, Roberts JD, Zakour RA. Rapid and efficient site-specific mutagenesis without phenotypic selection. Method Enzymol. 1987; 154:367–382.
50. Lee R, Kaushik N, Modak MJ, Vinayak R, Pandey VN. Polyamide nucleic acid targeted to the primer binding site of the HIV-1 RNA genome blocks in vitro HIV-1 reverse transcription. Biochemistry. 1998; 37:900–910. [PubMed: 9454580]
51. Misra HS, Pandey PK, Pandey VN. Polyamide nucleic acid targeted to the primer binding site of the HIV-1 RNA genome blocks in vitro HIV-1 reverse transcription. J Biol Chem. 1998; 273:9785–9789. [PubMed: 9545316]
52. Ausubel, FM.; Brent, R.; Kingston, RE.; Moore, DD.; Seidman, JS.; Smith, JA.; Struhl, K. Current protocols in Molecular Biology. Greene Publishing Associates and Wiley-Intersciences, John Wiley & Sons; New York: 1987.
53. Sanger F, Nicklen S, Coulson AR. DNA sequencing with chain-terminating inhibitors. Proc Natl Acad Sci USA. 1977; 74:5463–5467. [PubMed: 271968]
54. Segel, Irwin H. Enzyme Kinetics: Behavior and analysis of rapid equilibrium and steady state enzyme systems. John Wiley and Sons; NY: 1993.
55. Larder BA, Kemp SD, Harrigan PR. Potential mechanism for sustained antiretroviral efficacy of AZT-3TC combination therapy. Science. 1995; 269:696–699. [PubMed: 7542804]
56. Rubinek T, Bakhanashvili M, Taube R, Avidan O, Hizi A. The fidelity of 3′ misinsertion and mispair extension during DNA synthesis exhibited by two drug-resistant mutants of the reverse transcriptase of human immunodeficiency virus type 1 with Leu74Val and Glu89Gly. Eur J Biochem. 1997; 247:238–247. [PubMed: 9249032]

57. Bakhanashvili M, Avidon O, Hizi A. Mutational studies of human immunodeficiency virus type 1 reverse transcriptase: the involvement of residues 183 and 184 in the fidelity of DNA synthesis. FEBS Letters. 1996; 391:257–262. [PubMed: 8764985]
58. Arion D, Kaushik N, McCormick S, Borkow G, Parniak MA. Phenotypic Mechanism of HIV-1 Resistance to 3′-Azido-3′-deoxythymidine (AZT): Increased Polymerization Processivity and Enhanced Sensitivity to Pyrophosphate of the Mutant Viral Reverse Transcriptase. Biochemistry. 1998; 37:15908–15917. [PubMed: 9843396]
59. Canard B, Sarfati SR, Richardson CC. Enhanced binding of azidothymidine-resistant human immunodeficiency virus 1 reverse transcriptase to the 3′-azido-3′-deoxythymidine 5′-monophosphate-terminated primer. J Biol Chem. 1998; 273:14596–14604. [PubMed: 9603976]
60. Quan Y, Inouye P, Liang C, Rong L, Gotte M, Wainberg MA. Dominance of the E89G substitution in HIV-1 reverse transcriptase in regard to increased polymerase processivity and patterns of pausing. J Biol Chem. 1998; 273:21918–21925. [PubMed: 9705331]
61. Tachedjian G, Mellors J, Bazmi H, Birch C, Mills J. Zidovudine resistance is suppressed by mutations conferring resistance of human immunodeficiency virus type 1 to foscarnet. J Virol. 1996; 70:7171–7181. [PubMed: 8794364]
62. Crumpacker CS. Ganciclovir. New Eng J Med. 1996; 335:721–729. [PubMed: 8786764]
63. Oberg B. Antiviral effects of phosphonoformate (PFA, foscarnet sodium). Pharmacol Ther. 1989; 40:213–285. [PubMed: 2543994]
64. Xiong Y, Eickbush TH. Origin and evolution of retroelements based upon their reverse transcriptase sequences. EMBO J. 1990; 9:3353–3362. [PubMed: 1698615]
65. Korber, B.; Kuiken, C.; Foley, B.; Hahn, B.; McCutchan, F.; Mellors, J.; Sodroski, J., editors. Human Retroviruses and AIDS. pub: Los Alamos National Laboratory; LA, New Mexico: 1998. p. 87545
66. Tachedjian G, Hooker DJ, Gurusinghe AD, Bazmi H, Deacon NJ, Mellors J, Birch C, Mills J. Characterization of foscarnet-resistant strains of human immunodeficiency virus type 1. Virology. 1995; 212:58–68. [PubMed: 7545854]
67. Ding J, Das K, Hsiou Y, Sarafianos SG, Clark AD Jr, Jacobo-Molina A, Tantillo C, Hughes SH, Arnold E. Structure and functional implications of the polymerase active site region in a complex of HIV-1 RT with a double-stranded DNA template-primer and an antibody Fab fragment at 2.8 A resolution. J Mol Biol. 1998; 284:1095–1111. [PubMed: 9837729]

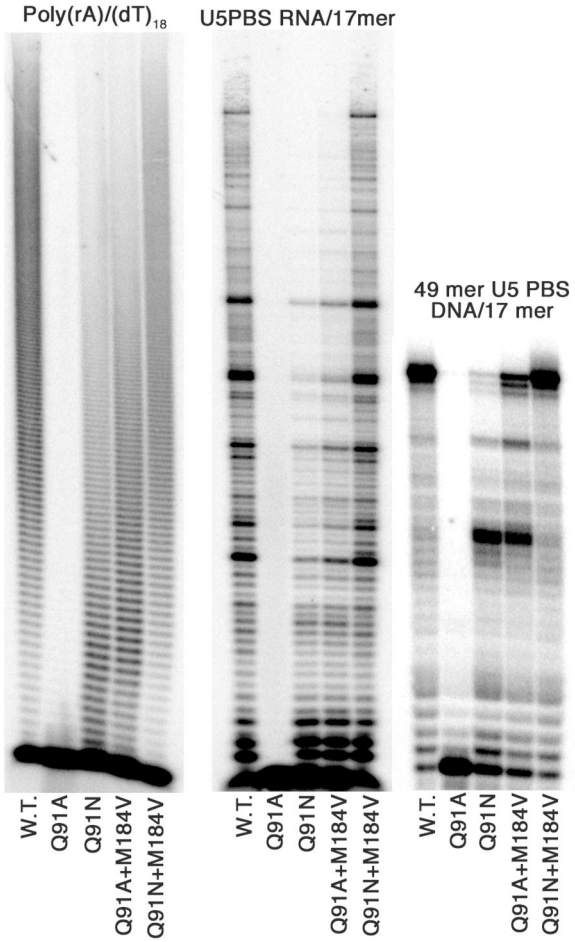

Figure 1. RNA- and DNA-directed DNA polymerase activity of WT HIV-1 RT and its mutant derivatives

Three template primers, poly (rA).$(dT)_{18}$, U5-PBS-RNA/17-mer DNA, and 49-mer U5-PBS DNA/17-mer DNA primer were used to assess the extension reaction catalyzed by the wild-type and mutant derivatives of HIV-1 RT. The primers labeled at the 5′ end with ^{32}P were annealed with the respective templates and used in the reactions carried out in a total volume of 6 μL. Reactions were quenched by the addition of Sanger's dye, then analyzed by 10% denaturing gel electrophoresis.

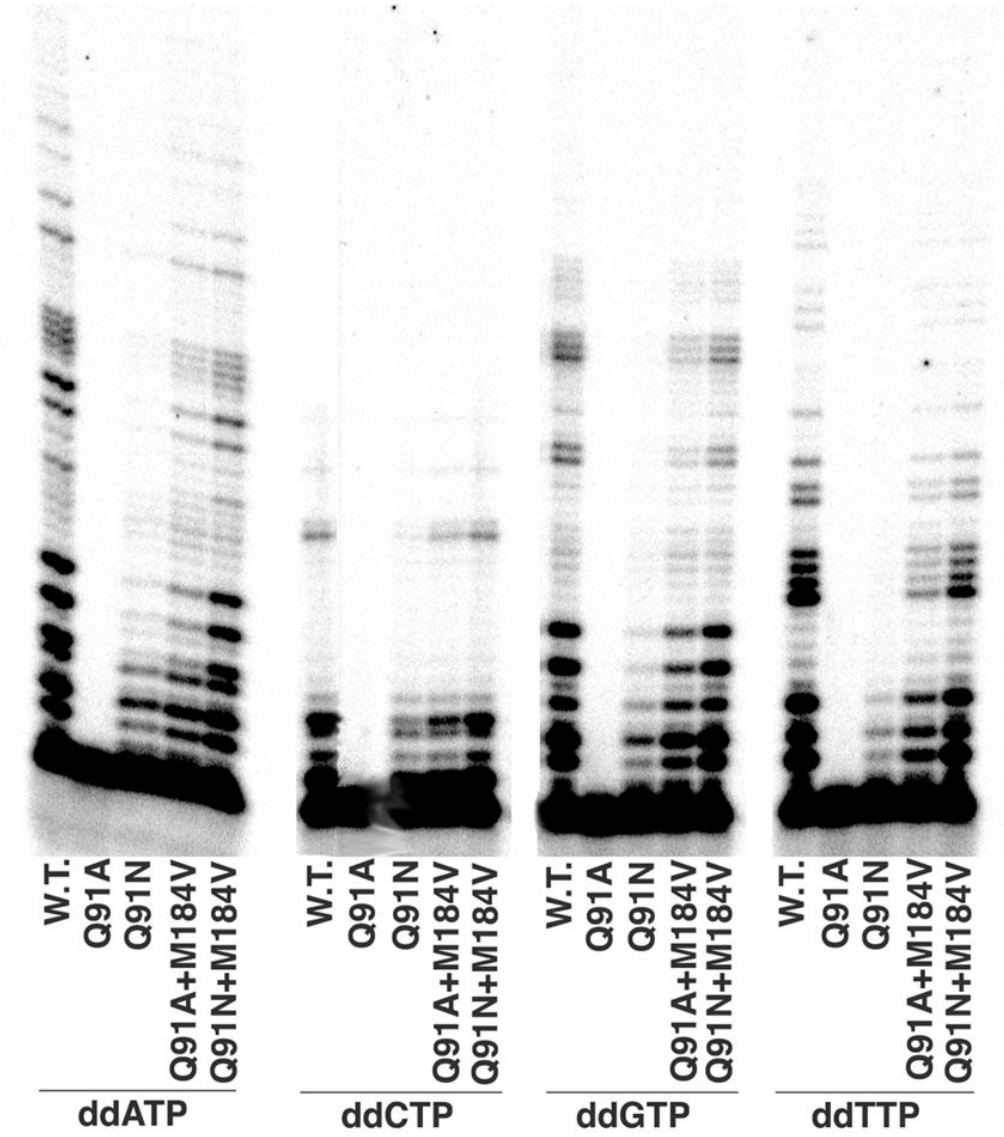

Figure 2. Sensitivity of WT HIV-1 RT and its mutant enzymes to dideoxy nucleoside triphosphate

The effect of ddNTPs on DNA synthesis catalyzed by wild-type and mutant enzymes was assessed on a U5-PBS-RNA template primed with $5'^{32}$-P-labeled 17-mer PBS primer. The concentration of dNTP was 10 μM; the concentration of each ddNTP was 5μM.

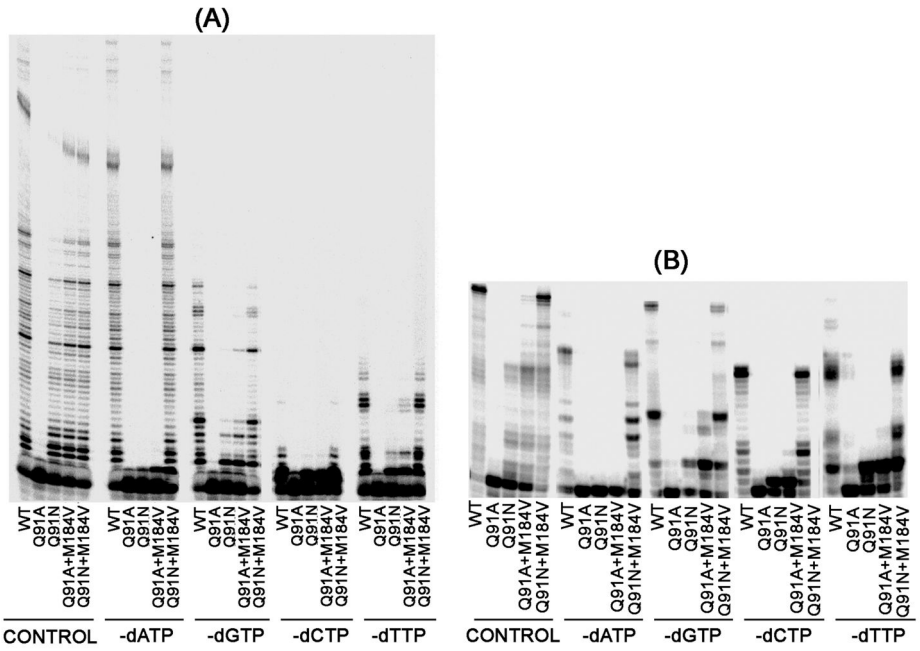

Figure 3. Misinsertion and mispair extension catalyzed by the wild-type enzyme and its mutant derivative in the absence of a single dNTP

Extension reactions were carried out on U5-PBS-RNA/17-mer DNA (A) and 49-mer U5-PBS DNA/17-mer DNA primer (B) in 6 μL reactions. These reactions were done at 25°C for 15 min in the presence of all four nucleotides (first set), in the absence of dATP (second set), in the absence of dGTP (third set), in the absence of dCTP (fourth set), and in the absence of dTTP (fifth set). The extension reactions were analyzed by 10% denaturing polyacrylamide gel electrophoresis.

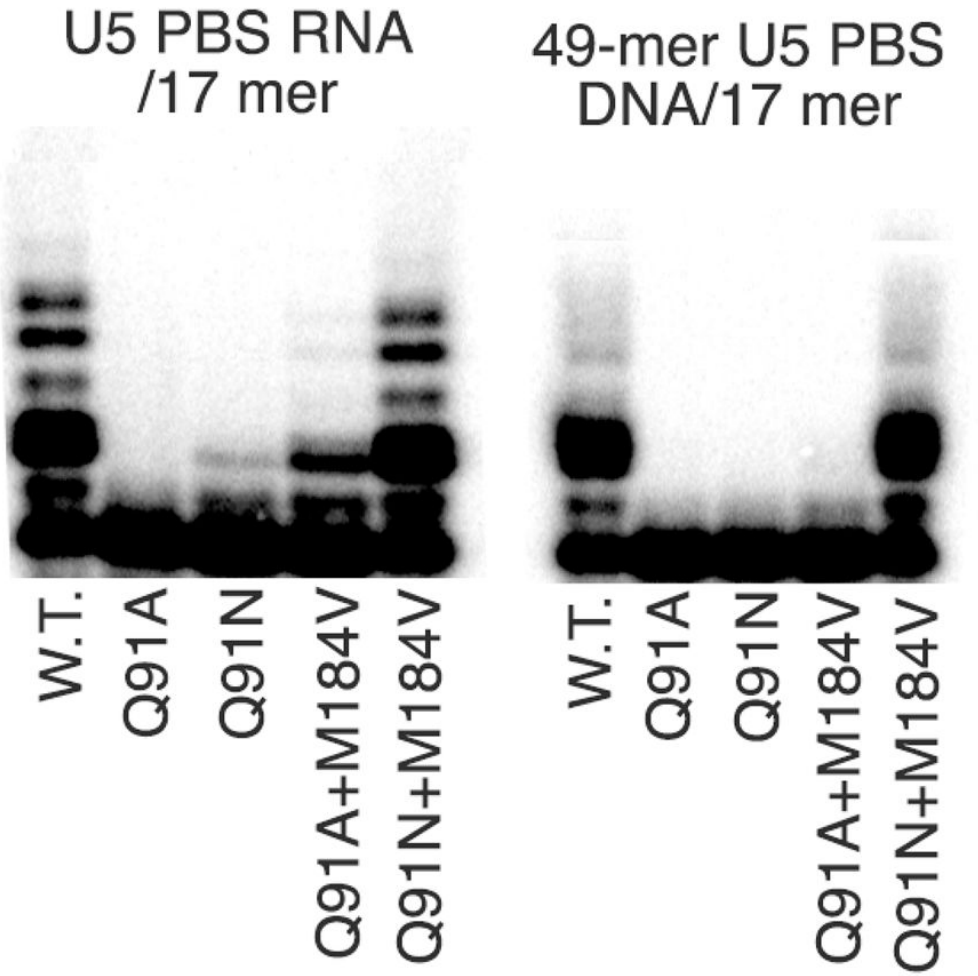

Figure 4. Use of rNTP in the extension reaction catalyzed by wild-type HIV-1 RT and its mutant derivatives

The ability of the RT enzymes to catalyze incorporation of rNTP substrates was examined using a U5-PBS-RNA template (panel A) and a 49-mer U5-PBS DNA template (panel B) annealed with 5′ ^{32}P labeled 17-mer primer. The extension reactions were done in the presence of 200 μM dNTP and 500 μM rNTP respectively. All reactions were carried out at 37°C for 5 min.

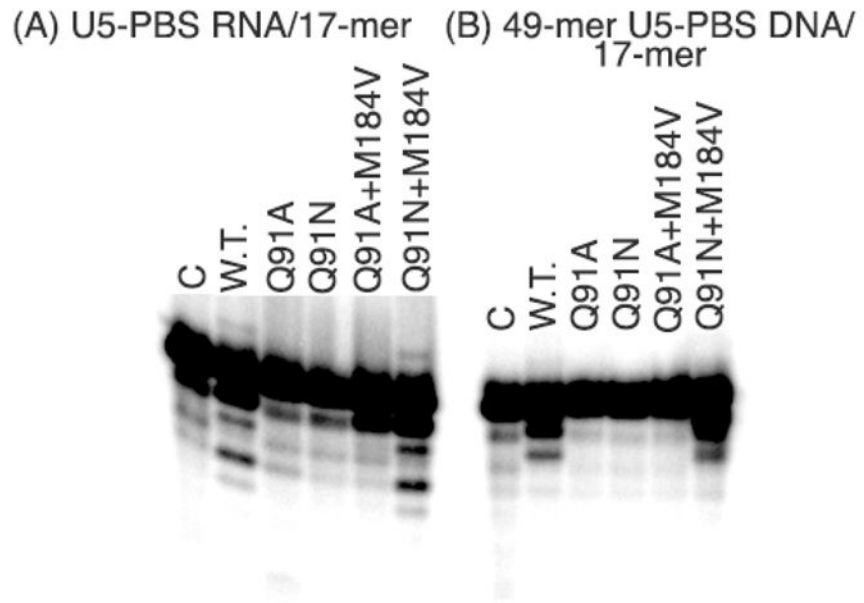

Figure 5. Pyrophosphorolysis reaction catalyzed by the wild-type enzyme and its mutant enzymes

The pyrophosphorolysis activity of the wild-type HIV-1 RT and its mutant derivatives was detected using both U5-PBS RNA (A) and heteropolymeric 49-mer U5-PBS DNA (B) templates primed with 17-mer 5′ ^{32} P- labeled DNA primer. The concentrations of pyrophosphate and Mg^{+2} in the reaction mixture were 0.5 mM and 2 mM, respectively. The reaction products were analyzed on denaturing polyacrylamide -urea gel as described previously.

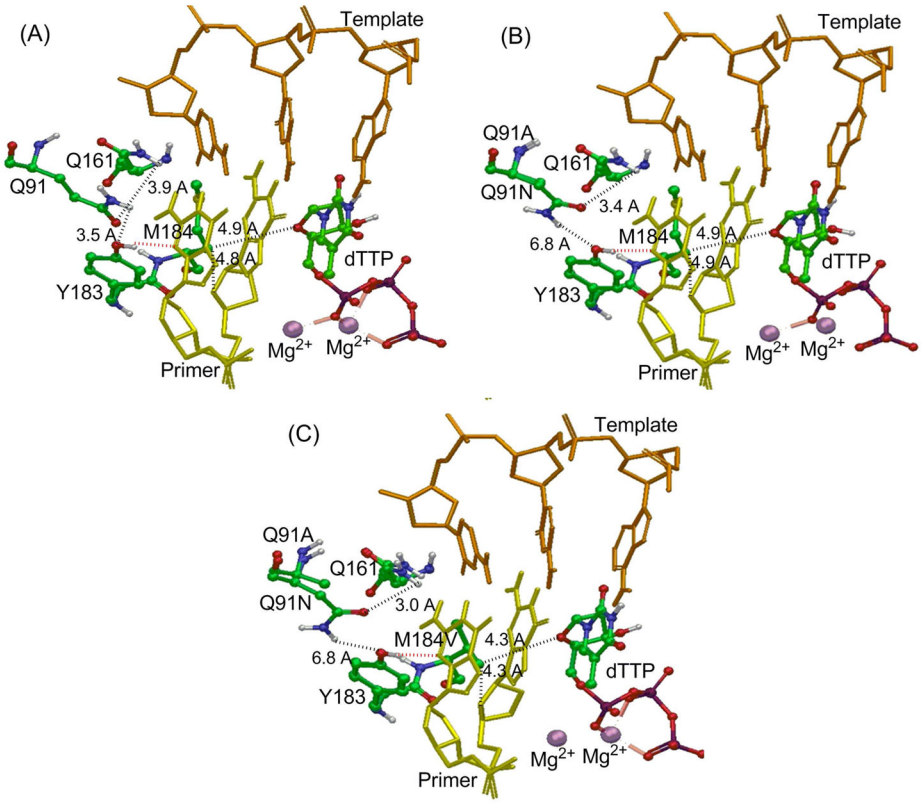

Fig 6. A 3 dimensional molecular model of the ternary complex of the wild type HIV-1 RT and its mutant derivatives

The molecular models of the ternary complexes of HIV-1 RT were generated using the coordinates of PDB ID: 1rtd. (A) Ternary complex structure of wild type enzyme, (B) overlaid single mutant derivatives, Q91A and Q91N, (C) overlaid double mutant derivatives Q91A/M184V and Q91N/M184V. Color scheme: Template is shown in orange, primer is shown in yellow, dTTP and amino acids are shown as balls and sticks with carbon in green, oxygen in red, nitrogen in blue, hydrogen in white, sulfur in yellow, phosphorous in purple, and Mg^{2+} in light pink. The hydrogen bonding interaction is shown by dotted red lines, whereas interacting distances in Å are shown as dotted black lines.

1. U5-PBS HIV-1 RNA containing the primer binding site

<----------PBS---------->

3'- CAG GGA CAA GCC CGC GGU GAC GAU CUC UAA AAG GUG UGA CUG AUU UUC CCA GAC UCC CUA GAG AUC AAU GGU CUC AGU GUG UUG UCU GCC CGU GUG UGA UGA ACU UCC UGA GUU CCG UUC GAA AUA ACU CCG AAU UCG UCA CCC AAG GGA UCA UCG GUC UCU CGA GGG UCC GAG UCU AGA-5'

2. 17-mer DNA PBS primer

5'-GTCCCTGTTCGGGCGCC-3'

3. Synthetic 30-mer RNA corresponding to U5-PBS RNA sequence

3'-CAGGGACAAGCCCGCGGUGACGAUCUCUAA-5'

4. 30-mer DNA complementary to 30-mer U5-PBS RNA

5'GTCCCTGTTCGGGCGCCACTGCTAGAGATT-3'

6. 49-mer U5-PBS DNA template corresponding to U5-PBS sequence

3'-CAG GGA CAA GCC CGC GGT GAC GAT CTC TAA AAG GTG TGA CTG ATT TTC C -5'

Chart 1.

Table 1

Polymerase activity of wild-type HIV-1 RT and its mutant derivatives [a]

Enzyme	U5-PBS RNA template/17-mer DNA primer	Poly rA.dT$_{18}$
WT	100	100
Q91A	8±2.5	12±1.5
Q91N	29±3.0	56±2.0
Q91A/M184V	60±1.5	70±1.4
Q91N/M184V	95±1.8	92±2.3

[a]The polymerase activity of the wild-type HIV-1 RT and its mutant derivatives was determined using the natural U5-PBS-RNA/17-mer template primer in the presence of Mg^{2+} as a divalent cation and saturated dNTP concentrations. Reactions were carried out at 37°C for 5 min. The total amount of picomol dNMP incorporated was determined as described in Materials and Methods.

Table 2

Steady-state kinetic parameters of the Wild-type HIV-1RT and its mutant derivatives [a]

Enzyme	Poly rA.dT $_{18}$ template -primer			Poly rC.dG$_{18}$ template-primer		
	K_{mdTTP} (μM)	K_{cat} (s^{-1})	K_{cat}/K_m ($M^{-1}s^{-1}$) ×10^5	K_{mdGTP} (μM)	K_{cat} (s^{-1})	K_{cat}/K_m ($M^{-1}s^{-1}$) ×10^5
WT	3.0±1.1	0.39±0.6	1.30	6.0±1.4	0.15±0.019	0.25
Q91A	30.0±3.5	0.10±0.03	0.03	25.0±4.0	0.02±0.006	0.008
Q91N	7.0±1.5	0.25±0.08	0.36	8.0±2.1	0.02±0.002	0.03
Q91A+M184V	37.0±4.0	0.23±0.07	0.06	57.0±5.0	0.06±0.010	0.01
Q91N+M184V	5.0±1.0	0.27±0.11	0.54	8.0±1.8	0.04±0.012	0.05
M184V	3.5±1.2	0.53±0.12	1.50	8.0±2.2	0.08±0.011	0.10

[a]The steady-state kinetic parameters for wild-type HIV-1 RT and its mutant derivatives were measured with indicated template-primers and corresponding dNTP substrate as described in the Materials and Methods. These determinations were carried out at sub saturating concentrations of the respective dNTP substrates.

Table 3

Inhibition of the Reverse Transcription Reaction of the Wild Type HIV-1 RT and the Mutant Derivatives of Q151 by ddNTP Inhibitors [a]

Enzyme	ddTTP		ddGTP	
	Ki (nM)	IC_{50} (nM)	Ki (nM)	IC_{50} (nM)
WT	4.0	17.0	112	308.0
Q91A	76.0	101.0	885	1239.0
Q91N	62.0	150.0	476	1094.0
Q91A+M184V	45.0	57.0	418	491.0
Q91N+M184V	12.0	36.0	130	285.0
M184V	18.0	69.0	403	900.0

[a] The inhibition assays and determination of the inhibitor constant (Ki) and half-maximal inhibitory constant (IC_{50}) for ddTTP and ddGTP were performed as described in Methods. Reactions were carried out at varying concentrations of the inhibitor while the concentrations of the normal dNTPs were kept constant at 10 μM.